Dynamic force microscopy analysis of block copolymers: beyond imaging the morphology

Philippe Leclère, F. Dubourg, Sophie Marsaudon, J. L. Bredas, R. Lazzaroni, Jean-Pierre Aimé

Dynamic force microscopy analysis of block copolymers: beyond imaging the morphology

Ph. Leclère[a,*], F. Dubourg[b], S. Kopp-Marsaudon[b], J.L. Brédas[a,c], R. Lazzaroni[a], J.P. Aimé[b]

[a]*Service de Chimie des Matériaux Nouveaux, Centre de Recherche en Science des Matériaux Polymères (CRESMAP), Université de Mons-Hainaut, Place du Parc 20, B-7000 Mons, Belgium*

[b]*CPMOH, Université de Bordeaux I, 351 Cours de la Libération, F-33405 Talence Cedex, France*

[c] *Department of Chemitry, The Univerity of Arizona, Tucon, AZ 85721-0041, USA*

Dynamic force microscopy is known for its ability to image soft materials without inducing severe damage. For such materials, the determination of the relative contributions of the topography and the local mechanical properties to the recorded image is of primary importance. In this paper, we show that a systematic comparison between images and approach–retract curve data allows the origin of the contrast to be straightforwardly evaluated. The method provides an unambiguous quantitative measurement of the contribution of the local mechanical response to the image. To achieve this goal, experimental results are recorded on a model system, a symmetric triblock copolymer, which possesses a lamellar morphology due to nanophase separation between elastomer and glassy domains. In this particular case, we show that most of the contrast in the height and phase images is due to variations of the local mechanical properties. As a step further, the analysis of the variation of the phase is carried out as a function of the tip–surface distance. Local variations of the phase can be linked to dissipative processes between the tip and the soft sample. When the tip touches the surface, viscous forces acting against the tip motion contribute to the phase lag. Depending on the tip apex geometry and on the nature of the sample, the relationships between the phase variations and the tip–surface distance can be derived. On that basis, we propose an approach to evaluate the viscosity at the nanometer scale.

Keywords: Scanning probe microscopy; Block copolymer; Phase separation; Mechanical properties

1. Introduction

The development of nanotechnologies and nanoscience implies a large effort to study and understand physical phenomena at the nanometer scale. Methods using local force probes provide important contributions to those studies, thanks to the small size of the tip. Among them, dynamical force techniques, i.e., using an oscillating probe, are particularly well adapted to soft samples such as polymers or biological systems. A convincing illustration of the potential of such dynamical methods is given by the good contrast of phase images on block copolymers in tapping-mode atomic force microscopy [1–7].

In dynamical modes, two types of operations are possible: either the oscillating amplitude is fixed and

* Corresponding author. Tel.: +32-65-37-38-68; fax: +32-65-37-38-61.
E-mail address: philippe@averell.umh.ac.be (Ph. Leclère).

the output signal is the resonance frequency (this is called the non-contact resonant force mode [8]), or the oscillation frequency is fixed and the variation of the amplitude and phase are recorded. This mode is commonly named tapping-mode (also known as intermittent contact mode [9]) and is the one that is considered in this study. Tapping-mode (TMAFM) is commonly used because of its ability to probe soft samples, due to the minimization of sample damage during the scans. Moreover, tapping-mode images can be of two different types: in one type, the image corresponds to the changes of the piezoactuator height necessary to maintain a fixed oscillation amplitude through a feedback loop (the height image); in the other type, the image contains the changes of the oscillator phase delay relative to the excitation signal (phase image). This additional imaging possibility has revealed in many cases a high sensitivity to variations of the local properties. A number of studies have shown the possibility to extract useful information from tapping-mode images of soft samples, especially with samples showing a particular contrast at small scale like blends of hard and soft materials [5,10].

Nevertheless, important questions remain about the physical origin of the image contrast in tapping-mode [11–14]. In many cases, the height images are considered to display topographic information, but it must be kept in mind that the local mechanical properties of the samples (i.e., the possibility that the tip slightly penetrates the surface) may also contribute to contrast in the height image. For the phase image, in the dominant repulsive regime [15], the phase shifts are related to the local mechanical properties. At this point, it is worth to mention that, in order to keep a well-defined oscillating behavior of the tip, the perturbation to the oscillator due to the contact with the surface is chosen to be small; in other words, the reduction of the free amplitude (the set-point) is only of a few percent. This method has two advantages: from an experimental point of view this allows to identify immediately hard and soft domains, the bright parts of the image corresponding to hard domains [5,6]. From a theoretical point of view, this allows us to use simple approximations providing analytical solutions able to fit the experimental data [5,15].

A key point for soft materials is a proper interpretation of the observed contrast. In most cases, one has to discriminate between the respective contributions of: (i) the topography and (ii) the different mechanical properties. In this paper, we propose a straightforward and easy experimental method to evaluate the contribution of the local mechanical properties to the image contrast. Our approach is based on the reconstruction of height or phase image sections via a rapid analysis of approach–retract curves recorded along those section lines. As recently described [5], a simple comparison between recorded images and the set of approach–retract curves provides an easy way to discriminate between the topographic and mechanical contributions. In the present paper, a step further in the understanding of the image contrast is proposed, via the analysis of the variation of the phase as a function of the tip–surface distance.

The local variations of the phase can be linked to dissipative processes between the tip and the sample [11–14]. When the tip touches the surface, viscous forces acting against the tip motion also contribute to the oscillator phase lag. Depending on the tip apex geometry and on the nature of the sample, the relationships between the phase variations and the tip–surface distance follow different laws [16].

As a final goal in this study, we try to evaluate the viscosity at the nanometer scale. For this purpose, we investigate a sample for which variations of the viscosity are expected within nanometer distances. The system is a thin film of a thermoplastic elastomer, i.e., a block copolymer in which the chemical structure of the sequences is designed in such a way that (i) phase separation of the sequences occurs, giving a well-defined spatial distribution of domains at the nanometer scale and (ii) the domains containing different sequences possess different mechanical properties [5,6]. Here, the chemical composition has been selected to produce a lamellar morphology. In this case, AFM pictures present an alternating array of rubbery and glassy lamellae, with a periodicity of 27 nm, as shown in Fig. 1.

After a brief description of the model used, the experimental conditions are described, along with the data treatment. Then a comparison between experimental and theoretical phase variations with tip–surface distance is given, followed by a discussion on the oscillator local sensitivity to phase variations. Besides the dissipation due to viscous forces, it is necessary to take into account a dissipation contribution coming from the sample viscoelastic response to van der

Fig. 1. Tapping-mode AFM phase image (1.0×1.0 μm^2) of a PMMA-*b*-P*n*Bua-*b*-PMMA film. The periodicity of the lamellar morphology is 27 nm.

Waals attractive forces [17,18]. This particular aspect, which is necessary from a practical point of view but complicates the analysis, is detailed in Ref. [16].

2. Methodology

2.1. Theoretical approach

The analysis is based on the use of the Navier–Stokes equation. Because the size of the tip is small, the inertial convective term can be neglected. For the same reasons, in spite of the high frequency used (few hundred kilohertzs), the small size of the tip implies that the non-stationary contribution is negligible. Therefore, only the viscous force contributes and the Navier–Stokes equation reduces to the Stokes equation: $\vec{\nabla}\vec{p} = \eta\Delta\vec{v}$. From this equation, we know that the viscous force acting on a solid with a characteristic length ϕ moving with velocity $\vec{v}$ in a fluid with a viscosity η will be of the form $\vec{F} \propto \eta\phi\vec{v}$.

For tapping-mode experiments, the tip geometry and the local sample viscosity η are the two key parameters. As the tip geometry and size are always difficult to assess in local force probe methods, we have chosen to describe two extreme experimental situations, as sketched in Fig. 2:

(a) A spherical tip apex partially immersed into the fluid (i.e., the polymer under study here), providing a viscous force acting on the tip given by:

$$\vec{F}_{\mathrm{Sph}} = 3\pi\eta\delta\vec{v}$$

with δ the indentation of the tip into the sample. Note that in this case, the force is independent of the tip radius.

(b) A high aspect ratio tip with indentation δ into the sample and radius r at the sample surface, giving the following viscous force acting on the tip:

$$\vec{F}_{\mathrm{Needle}} = \frac{6}{5}\pi\eta r\left(4 + \frac{\delta}{r}\right)\vec{v}$$

In the latter expression, note that if $\delta \ll r$, F is independent on the indentation. This is similar to the case of a cylinder with a small indentation for which one has $\vec{F}_{\mathrm{Cyl}} \propto \eta\rho\vec{v}$ with ρ the cylinder radius.

For the second important parameter, the sample viscosity at this small scale, Brochard Wyart and de Gennes [19] have discussed the viscosity dependence

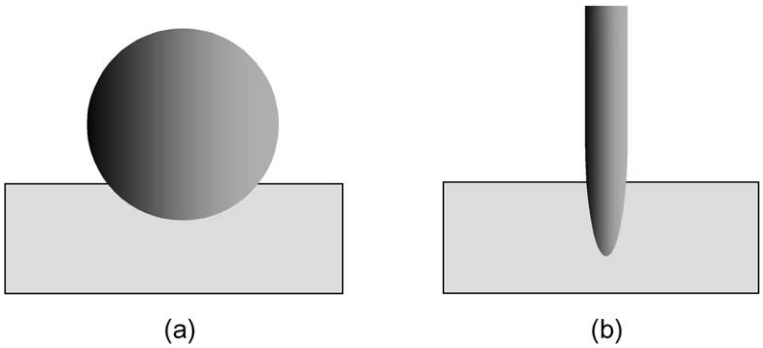

Fig. 2. Sketch of the tip geometries: (a) spherical tip; (b) needle-like tip.

on the size ϕ of an ultra-small particle testing a polymer melt. Following Rouse theory, they have proposed a viscosity scaling law for $a < \phi < d_t$, where a is the monomer size and d_t the Edwards tube diameter describing the entanglements effects. Including the viscosity scaling law into the force expressions gives:

(a) For the spherical tip of radius R:

$$\vec{F}_{\text{Sph}}^{\text{Rouse}} = 3\pi\eta_m R(\delta/a)^2\vec{v}$$

where η_m is the monomer viscosity.

(b) For the needle-like tip:

$$\vec{F}_{\text{Sph}}^{\text{Rouse}} = (6/5)\pi\eta_m(r/a)^2(4 + (\delta/r))\vec{v}$$

For this case, the variation of the force with δ is independent of the existence of scaling effects of the viscosity. The only difference will be that the exact value of r/a (typically around 10) introduces a factor of 100 between the viscosity value with or without scaling effects.

With the dynamical tapping-mode, the measured quantities are the oscillator amplitude and phase variations with the tip–sample displacement. To transform the viscous force into oscillator phase expressions, we follow the analytical approach based on the variational principle detailed elsewhere [20]. From these equations, we propose to estimate the viscosity at the local scale.

2.2. Experimental

The sample used in this study is a symmetric triblock copolymer used as thermoplastic elastomer: it is made of a rubbery (poly(*n*-butyl acrylate)) inner sequence (i.e., its glass transition temperature is below room temperature) and two symmetrical thermoplastic (poly(methyl methacrylate)) outer blocks (i.e., their glass transition temperature is well above room temperature).

The copolymer films are prepared from a toluene solution (2 mg/ml), deposited on freshly cleaved mica and slowly evaporated in a solvent saturated atmosphere. The films are then annealed at 140 °C in vacuum. The resulting films have a thickness of about 500 nm, with a well-defined lamellar organization (Fig. 1). This copolymer surface has been shown to be topographically flat by two different local force probe experiments [5,6,21]. The contrast in the figure is due to local differences in the sample mechanical properties: for a given image amplitude, the tip indents more into the elastomeric domains than into the glassy ones.

The scanning probe experiments are performed in a glove box (in order to reach oxygen and water concentrations lower than 1 ppm and therefore ensure stability of the experimental conditions) with a Nanoscope IIIa (from Digital Instruments) operating in tapping-mode. The tip is a commercial silicon tip (TESP-NCL-W, with a stiffness k_c of about 45 N m^{-1}). The oscillator characteristics (amplitude and phase variations with frequency) are measured at ca. 600 nm from the surface from time to time during the experiment. The quality factor Q is 470.

Approach–retract curves (variations of the oscillator amplitude A and phase delay φ with the piezoceramic height) are measured at different surface locations. Typical conditions are 20 nm vertical scans

with a scan rate of 0.5 Hz. The oscillation frequency is set at a value slightly smaller than the resonance frequency. At this frequency, the contact point is set during the bifurcation of the oscillator when the attractive interaction between the tip and the sample becomes large enough to modify the oscillator behavior [18,20]. This procedure reduces the error made on the determination of the vertical origin, since the jump occurs within 0.2 nm thus a relative error of about 0.4%. At this contact point, the oscillator amplitude abruptly increases when the tip is at about 1 nm from the surface, thus helping to locate the sample surface. The value of the free amplitude A_f is 55 nm (A_f is the value of the oscillation amplitude at large distance from the sample). The value of the resonance amplitude A_0 is equal to 79 nm.

2.3. Tapping-mode image reconstruction

For the tapping-mode image reconstruction, the approach–retract curves are recorded (Fig. 3), then analyzed. The first step is to adjust D_{bif}, i.e., the distance at which the oscillator bifurcates, at the same vertical position value for all the approach–retract curves. Such an adjustment assumes a similar tip–sample attractive interaction for all domains, as discussed below. The D_{bif} adjustment allows us to extract selectively the mechanical part that participates in the contrast among the different domains; therefore it provides a quantitative measurement of the mechanical contribution to the contrast.

Typical experimental approach curves are shown for the amplitude variation (Fig. 3a) and for the phase variation (Fig. 3b). Approach–retract curves recorded on different domains on the sample surface are different: the slope of the amplitude is 0.75 for the harder glassy domains (gray curve), while it is smaller (0.60) on the elastomer domains, meaning that, for the same set-point, there is larger tip indentation in the elastomer domain (black curve).

From the amplitude curve, one then checks the vertical position Z_i corresponding to the image fixed amplitude A_i (the set-point). Then, from the phase curve, one obtains the corresponding phase noted φ_i. This operation is repeated for all the positions along the scan direction (here the *Y*-direction): Z_i and φ_i values are thus recorded for all *Y* positions for which the approach–retract curves are measured. Plots of

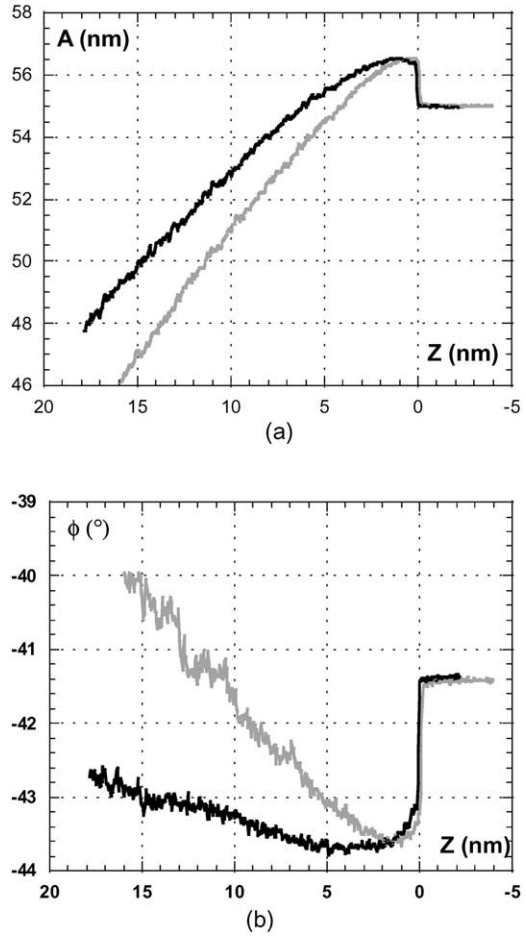

Fig. 3. Experimental approach–retract curves recorded on the block copolymer: (a) amplitude data; (b) phase data. The black curves correspond to the rubbery lamellae while the gray curves correspond to the glassy lamellae.

the piezoactuator heights (Z_i) and phases (φ_i) versus *Y* sample locations are obtained, which are then compared with the corresponding sections of the tapping-mode height and phase images (Fig. 4). The correspondence between the two sets of data (tapping height or phase images and approach–retract analysis) appears to be very good. This agreement means that for those copolymers, the contrast in the height image is related to different oscillator responses on the glassy and elastomer domains, with no discernible topographic contribution to the contrast. Therefore, the contrast is mostly due to changes in the sample local mechanical properties.

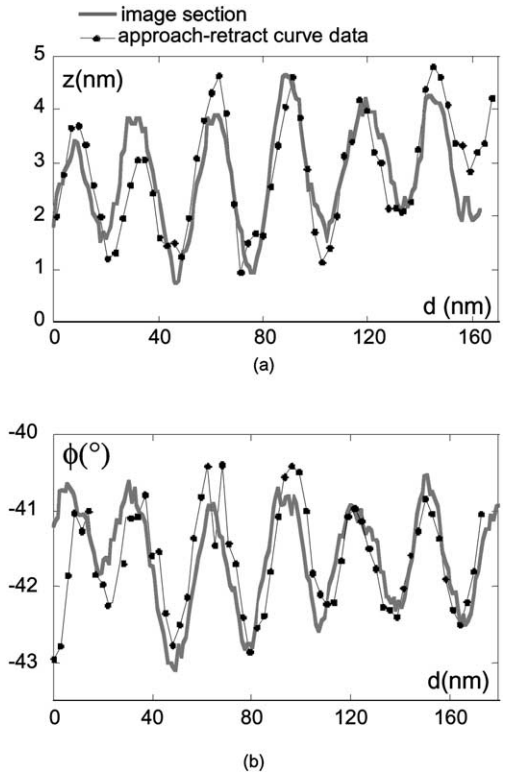

Fig. 4. Comparison of the image sections with the profiles built from the approach–retract curves data: (a) amplitude data; (b) phase data.

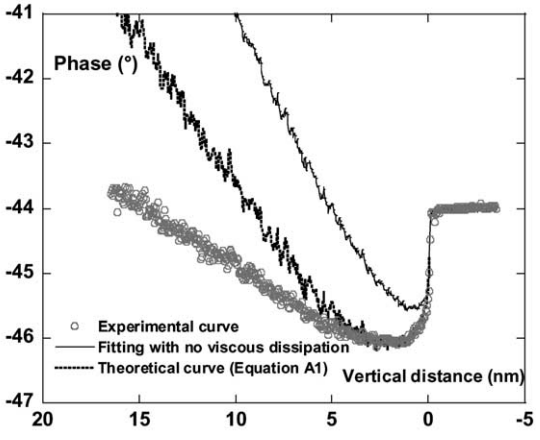

Fig. 5. Comparison of the experimental data obtained with two theoretical expressions corresponding to: no viscous dissipation (thin full line); and a viscous force independent of the indentation depth (black dotted line, Eq. (A.1)).

2.4. Fitting of the phase variation with distance

To understand the origin of the contrast, we can reproduce the phase variations for the different domains with the adapted analytical expression, as described in Appendix A.

For the fits, the phase is systematically set such that the free phase verifies exactly the usual phase value of a damped harmonic oscillator: $\sin\varphi = -u(A_f/A_0)$, where u is the reduced frequency ν_-/ν_0. The formula used for the fit is given in Ref. [16] and in Appendix A. In this fit, two parameters are used: the non-contact dissipation (γ_{NC}), and the dissipation due to viscous forces (γ_{visc}). The fit for the phase evaluation uses the recorded experimental variation of the amplitude $A(D)$, where D is the cantilever–surface distance.

2.4.1. No viscous force and viscous force independent of the indentation

Fig. 5 gives a comparison of the experimental phase curve obtained on one area with two theoretical phase curves:

(a) One is obtained assuming no viscous dissipation (thin black line): as expected, the dissipation of the oscillator in air (i.e., in the absence of any viscous force) cannot describe the experimental data. Note that the bumpiness of the calculated curve is due to the use of the experimental amplitude data for the fitting.

(b) The second curve is obtained by assuming a viscous force independent of the indentation δ (black dotted line). Whatever the value of the viscosity and the non-contact dissipation parameters, the calculated curves are unable to reproduce the experimental phase variations. It is thus clear that the phase variations cannot be understood assuming that the viscous force is independent of the indentation δ, which corresponds to the case of an ultra-thin tip or a cylinder shape for an indentation smaller than the radius [16,19].

2.4.2. Viscous force varying linearly with the indentation depth δ

Fig. 6 shows the fits obtained from expression (A.2), assuming a non-contact dissipation plus a viscous force varying linearly with the indentation depth δ. The experimental phase variations are rather well

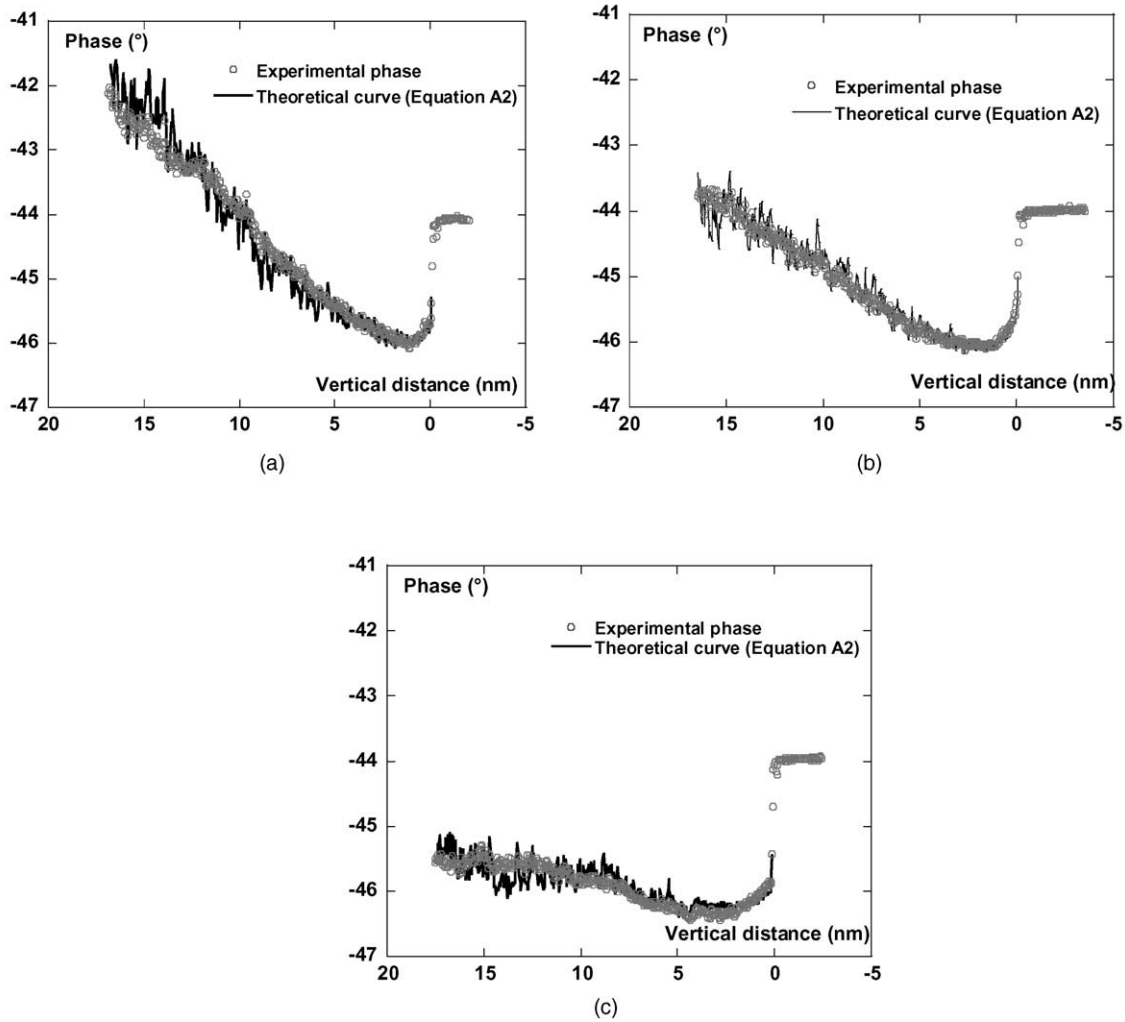

Fig. 6. Comparison of the experimental data obtained on three different areas considering a viscous force proportional to the indentation depth (Eq. (A.2)): (a) for the glassy lamella; (b) for the intermediate domain; (c) for the rubbery lamella.

reproduced. Such a good agreement means that the phase contrast obtained on different domains on the copolymer can be explained with a viscous force acting on a spherical tip apex partially immersed into the sample described as a medium with a viscosity independent of the indentation depth [16].

The non-contact dissipation term of Eq. (A.2) mainly gives a phase offset since it does not depend on the indentation. From the fit, it is possible to evaluate the contribution of the non-contact damping and of the viscous damping. At the very beginning of the approach (which corresponds to small indentations), the non-contact damping is superior to the viscous one. At larger indentations (superior to 2.5 nm), the non-contact damping is small as compared to the viscous damping.

2.4.3. Viscous force varying as δ^2

Fig. 7 shows the results obtained by considering a viscous force proportional to δ^2. While the oscillator phase variation on the glassy part might be approximately described by (A.3), the fit is poor for the intermediate and rubbery domains. Therefore, the oscillator phase variations with distance in the present experiment cannot be described with the analytical model using Rouse dynamics [16,19].

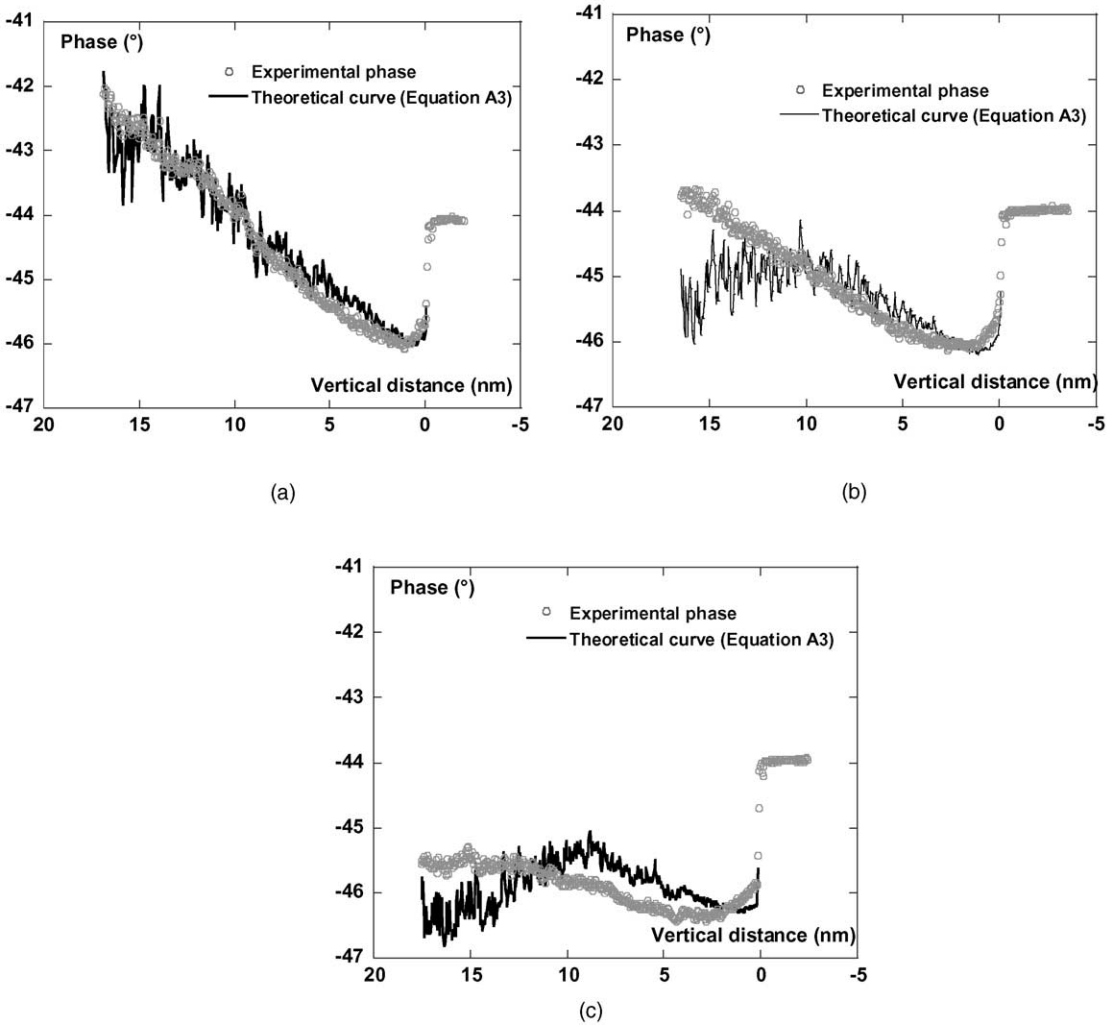

Fig. 7. Comparison of the experimental data obtained on the three types of domains with the theoretical expression (A.3) considering a viscous force varying as δ^2. The fits are unsuccessful for the intermediate and rubbery domains.

The experimental data thus allow us to discriminate among the different laws of phase variation with distance given in Ref. [16]: the only expression allowing to fit the experimental phase is Eq. (A.2) assuming a spherical tip embedded in a liquid with a viscosity independent of the indentation depth. If one aims at evaluating the viscosity, the great advantage of this law of phase variation is that it is independent of the tip radius value.

To evaluate the lateral sensitivity of the oscillator, approach–retract curves can be recorded on many close locations (for example on a line) and then fitted. The resolution will then be given by the capacity to differentiate between adjacent points. The fit has been carried out for different areas along the line shown in the phase image of Fig. 8. The corresponding variations of the fit parameters are displayed in Fig. 9, together with the phase image section. The viscosity values obtained from the fit follow approximately the phase variation of the image. This relates the phase contrast of the image to viscous forces acting on the tip.

Moreover, the robustness of the viscosity variations with the type of domain, i.e., with the sample local mechanical properties, allows us to evaluate the oscillator ability to discriminate local variations of viscosity.

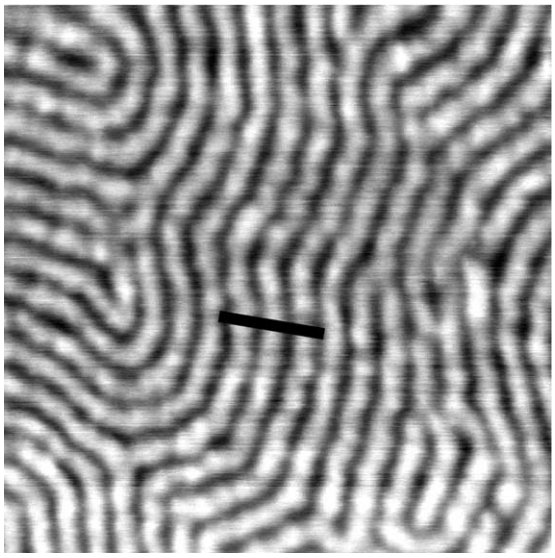

Fig. 8. Phase image of the copolymer ($500 \times 500\ \mathrm{nm}^2$). The fits are carried out on data recorded along the black line.

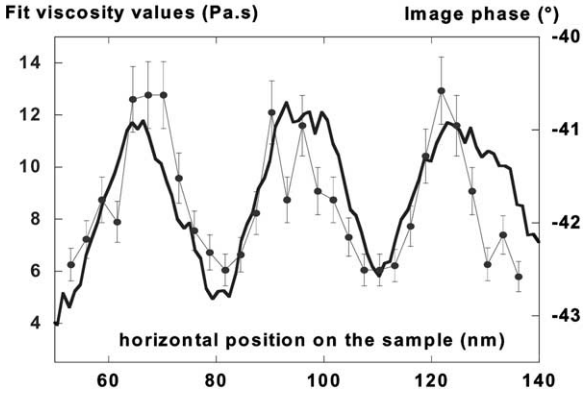

Fig. 9. Comparison of the phase image section and the local viscosity values obtained from the fit. The values follow the same variations as the phase image contrast, thus reproducing the local variations of the mechanical properties.

Variations of viscosity values are detectable within the distance between two adjacent locations from the approach–retract curves. The lateral resolution of those data is thus about 3 nm.

3. Conclusions

From tapping-mode images of a block copolymer, it is not only possible to describe the morphology corresponding to the nanophase separation occurring between the specific domains but also to evaluate accurately the respective contributions of the topography and the mechanical properties. Here, we propose that the phase contrast can be explained on the basis of the viscous forces acting against the tip motion during the indentation of the tip in the sample.

The experimental data obtained on the lamellar copolymer morphology have shown that:

(a) it is possible to discriminate among the different viscous regimes predicted from the experimental data;
(b) the oscillator sensitivity is sufficient to detect viscosity variations within a lateral distance of few nanometers;
(c) the viscosity values derived from the fits are compatible with the assumptions of the theoretical model.

In particular, the phase variations with distance can be understood with a viscous force varying linearly with indentation, corresponding to a hemispherical tip partially embedded in the polymer film. The consequence of this phase variation law is that the viscosity measurement is independent of the tip radius, which allows one to make quantitative measurements.

Acknowledgements

The authors are grateful to J.D. Tong and R. Jérôme (CERM, University of Liège, Belgium) for the synthesis of the triblock copolymer. Research in Mons is partially supported by the Belgian Federal Government Office of Science Policy (SSTC) "*Pôle d'Attraction Interuniversitaire en Chimie Supramoléculaire et Catalyse Supramoléculaire*" (PAI 4/11), the European Commission and the Government of the Région Wallonne. Research in Bordeaux is supported by the Conseil Régional d'Aquitaine. RL is Directeur de Recherches du Fonds National de la Recherche Scientifique (FNRS-Belgium).

Appendix A

Here, we present the exact expressions for the fit as a function of the expression for the viscous force, as described in the text.

(a) For a viscous force independent of the indentation δ:

$$\varphi = \arcsin\left\{ -u\frac{A}{A_0}\left[1 + \frac{\gamma_{NC}}{\gamma_0} + \frac{24}{5}\frac{\eta R}{\gamma_0}\left(\frac{D}{A}\sqrt{\frac{A^2-D^2}{A^2}} + \arccos\left(\frac{D}{A}\right)\right)\right]\right\} \tag{A.1}$$

(b) For a viscous force linearly dependent on the indentation δ:

$$\varphi = \arcsin\left\{ -u\frac{A}{A_0}\left[1 + \frac{\gamma_{NC}}{\gamma_0} + \frac{\eta}{\gamma_0}\left(\sqrt{\frac{A^2-D^2}{A^2}}\left(\frac{D^2}{A}+2A\right) - 3D\arccos\left(\frac{D}{A}\right)\right)\right]\right\} \tag{A.2}$$

(c) For a viscous force quadratically dependent on the indentation δ:

$$\varphi = \arcsin\left\{ -u\frac{A}{A_0}\left[1 + \frac{\gamma_{NC}}{\gamma_0} + \frac{\eta}{5a^2\gamma_0}\left(\sqrt{\frac{A^2-D^2}{A^2}}\left(16A^3 + 130ADR + 83AD^2 + 6\frac{D^4}{A} + 20D^3\frac{R}{A}\right)\right.\right.\right.$$
$$\left.\left.\left. +15\arccos\left(\frac{D}{A}\right)(8RD^2 + 4D^3 + 2A^2R + 3A^2D)\right)\right]\right\}$$

References

[1] Ph. Leclère, R. Lazzaroni, J.L. Brédas, J.M. Yu, Ph. Dubois, R. Jérôme, Langmuir 12 (1996) 4317.

[2] W. Stocker, J. Beckmann, R. Stadler, J.P. Rabe, Macromolecules 29 (1996) 7502.

[3] S.N. Magonov, V. Elings, M.H. Wangbo, Surf. Sci. 389 (1997) 201.

[4] Ph. Leclère, G. Moineau, M. Minet, Ph. Dubois, R. Jérôme, J.L. Brédas, R. Lazzaroni, Langmuir 15 (1999) 3915.

[5] S. Kopp-Marsaudon, Ph. Leclère, F. Dubourg, R. Lazzaroni, J.P. Aimé, Langmuir 16 (2000) 8432.

[6] A. Rasmont, Ph. Leclère, C. Doneux, G. Lambin, J.D. Tong, R. Jérôme, J.L. Brédas, R. Lazzaroni, Colloids Surf. B 19 (2000) 381.

[7] M. Konrad, A. Knoll, G. Krausch, R. Magerle, Macromolecules 33 (2000) 5518.

[8] T.R. Albrecht, P. Grütter, D. Horne, D. Rugard, J. Appl. Phys. 69 (1991) 668.

[9] Q. Zhong, D. Inniss, K. Kjoller, V.B. Elings, Surf. Sci. 290 (1993) L688.

[10] A. Knoll, R. Magerle, G. Krausch, Macromolecules 34 (2001) 4159.

[11] J.P. Cleveland, B. Anczykowski, A.E. Schmid, V.B. Elings, Appl. Phys. Lett. 72 (1998) 2613.

[12] R. Garcia, A. San Paulo, Phys. Rev. B 60 (1999) 4961.

[13] F. Dubourg, G. Couturier, J.P. Aimé, S. Kopp-Marsaudon, Ph. Leclère, R. Lazzaroni, J. Salardenne, R. Boisgard, in: V.V. Tsukruk, N.D. Spencer (Eds.), Recent Advances in Scanning Probe Microscopy of Polymers, Macromolecular Symposia, 2001, pp. 167, 179.

[14] R. Boisgard, J.P. Aimé, G. Couturier, Appl. Surf. Sci. (2002).

[15] L. Nony, R. Boisgard, J.P. Aimé, J. Chem. Phys. 111 (1999) 1615.

[16] F. Dubourg, J.P. Aimé, S. Marsaudon, R. Boisgard, Ph. Leclère, Eur. Phys. J. E 6 (2001) 49.

[17] J.P. Aimé, D. Michel, R. Boisgard, L. Nony, Phys. Rev. B 59 (1999) 2407.

[18] J.P. Aimé, R. Boisgard, L. Nony, G. Couturier, J. Chem. Phys. 114 (2001) 4945.

[19] F. Brochard Wyart, P.G. de Gennes, Eur. Phys. J. E 1 (2000) 93.

[20] L. Nony, R. Boisgard, J.P. Aimé, J. Chem. Phys. 111 (1999) 1615.

[21] Ph. Leclère, A. Rasmont, J.P. Aimé, R. Jérôme, J.L. Brédas, R. Lazzaroni, in: V.V. Tsukruk, N.D. Spencer (Eds.), Recent Advances in Scanning Probe Microscopy of Polymers, Macromolecular Symposia, 2001, pp. 167, 119.